

Invariant yield and azimuthal anisotropy measurements of strange and multi-strange hadrons in Au+Au collision at $\sqrt{s_{NN}} = 27$ and 54.4 GeV at STAR

Prabhupada Dixit (for the STAR collaboration)*†

Indian Institute of Science Education and Research, Berhampur, India

E-mail: dixitprabhupada471@gmail.com

In this proceedings, we have presented the invariant yield measurements of strange and multi strange hadrons such as K_S^0 , Λ , $\bar{\Lambda}$, ϕ , Ξ^- , $\bar{\Xi}^+$, Ω^- , $\bar{\Omega}^+$ in Au+Au collisions at $\sqrt{s_{NN}} = 54.4$ GeV at midrapidity ($|y| < 0.5$). The second and third-order azimuthal anisotropic flow of the above mentioned particles at $\sqrt{s_{NN}} = 27$ and 54.4 GeV are also discussed. Some of the important observables such as nuclear modification factor (R_{CP}), baryon to meson ratio (Ω/ϕ), transverse momentum dependence of v_2 and v_3 are measured. The number of constituent quark (NCQ) scaling of v_2 and v_3 is studied for all these particles.

International conference on Critical Point and Onset of Deconfinement (CPOD)

15-19 March 2021

Online

*Speaker.

†A footnote may follow.

1. Introduction

Quantum chromodynamics predicts the existence of a deconfined state of quarks and gluons at high temperature and density. Heavy-ion collisions are a unique tool to create and study such a state of the matter. There are many observables to probe the QGP phase of the system created in heavy-ion collisions, some of them are nuclear modification factor, baryon to meson ratio, anisotropic flow.

The nuclear modification factor is the ratio of the particle yield in central to peripheral collisions scaled by the number of binary collisions which is given by

$$R_{CP} = \frac{[\frac{dN}{dp_T} \frac{1}{N_{coll}}]_{central}}{[\frac{dN}{dp_T} \frac{1}{N_{coll}}]_{peripheral}}. \quad (1.1)$$

Suppression of the ratio at high p_T indicates the energy loss by the high p_T partons inside colour field of the QGP medium. The baryon to meson ratio, Ω/ϕ , gives us information about the hadron formation mechanism during the hadronization. Another important observable to probe the QGP phase is anisotropic flow. Flow is defined as the collective expansion of the medium created in heavy-ion collisions. Depending on the initial spatial geometry and event-by-event fluctuations in the distribution of nucleons inside the colliding nuclei there can be the presence of different orders of anisotropy in the flow. It has been predicted by model calculations that anisotropic flow coefficients are sensitive to the equation of the state and shear viscosity to entropy density ratio (η/s) [1]. To study the flow, we use Fourier series expansion of the azimuthal distribution of the invariant yield given by

$$E \frac{d^3N}{dp^3} = \frac{1}{2\pi} \frac{d^2N}{p_T dp_T dy} \left[1 + \sum_n 2v_n \cos n(\phi - \Psi_R) \right]. \quad (1.2)$$

Here, v_1 , v_2 and v_3 represent directed flow, elliptic flow and triangular flow respectively. The n^{th} -order flow coefficient is given by

$$v_n = \langle \cos n(\phi - \Psi_n) \rangle, \quad (1.3)$$

where, Ψ_n is the n^{th} order event plane. A detailed description of event plane and its calculation can be found in Ref. [2].

We have used strange and multi-strange hadrons in our study since they are expected to freeze out earlier and have small hadronic interaction cross section [3] compared to other charged hadrons. So they get least affected by the late-stage hadronic interaction phase of the system.

2. Analysis details

Since the particles used in our analysis are short-lived and decay before reaching the detector, we have reconstructed them by using the invariant mass of their daughter particles. The decay channels and branching ratios of these particles are given below.

$$\begin{aligned}
K_S^0 &\rightarrow \pi^+ + \pi^- \text{ (B.R = 69.20\%)} \\
\Lambda(\bar{\Lambda}) &\rightarrow p(\bar{p}) + \pi^- (\pi^+) \text{ (B.R = 63.9\%)} \\
\Xi(\bar{\Xi}^+) &\rightarrow \Lambda(\bar{\Lambda}) + \pi^- (\pi^+) \text{ (B.R = 99.887\%)} \\
\Omega(\bar{\Omega}^+) &\rightarrow \Lambda(\bar{\Lambda}) + K^- (K^+) \text{ (B.R = 67.8\%)} \\
\phi &\rightarrow K^+ + K^- \text{ (B.R = 49.1\%)}
\end{aligned}$$

For particles like K_S^0 , Λ , Ξ and Ω weak decay topology cuts are applied to reduce the combinatorial background. For Λ hyperons weak decay feed-down correction is implemented. In the upper panel of Fig. 1, the invariant mass distribution is shown for K^+ and K^- to reconstruct the ϕ mesons as an example. The combinatorial background is calculated by event-mixing method and subtracted from the signal+background distribution to get the signal of ϕ mesons.

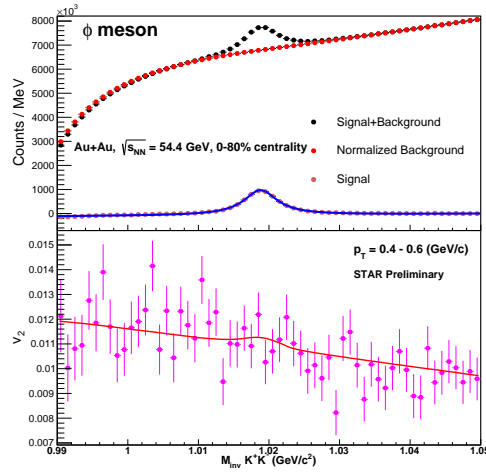


Figure 1: The upper panel shows the signal+background distribution and signal peak of phi meson in Au+Au collision at $\sqrt{s_{NN}} = 54.4$ GeV in p_T bin 0.4-0.6 GeV/c. The lower panel shows v_2 as a function of invariant mass of K^+ and K^- . The distribution is fitted with a function given in Eq. 2.1.

For flow coefficient measurements we have used invariant mass method [4]. As an example we have explain v_2 calculation of ϕ mesons using this method. In this method we need to calculate v_2 as a function of invariant mass of decay daughters, K^+ and K^- as shown in the lower panel of Fig. 1. The distribution is fitted with a function given in Eq. 2.1, where v_2^{S+B} is the combined v_2 of signal+background. v_2^S and v_2^B represent v_2 of signal and background respectively. v_2^B is parametrized as a first order polynomial of invariant mass. v_2^S is a free parameter and can be extracted from the fitting. Same method was used to calculate v_2 and v_3 of other particles as well.

$$v_2^{S+B}(M_{inv}) = v_2^S \frac{S}{S+B}(M_{inv}) + v_2^B \frac{B}{S+B}(M_{inv}). \quad (2.1)$$

3. Results and Discussion

Figure 2 shows the nuclear modification factor (R_{CP}) at $\sqrt{s_{NN}} = 54.4$ GeV, which is calculated by taking ratio of particle yields in 0-5% and 40-60% for K_S^0 , $\Lambda + \bar{\Lambda}$, $\Xi^- + \bar{\Xi}^+$ and for ϕ mesons. The ratio shows a strong suppression at high p_T indicating partonic energy loss inside the medium.

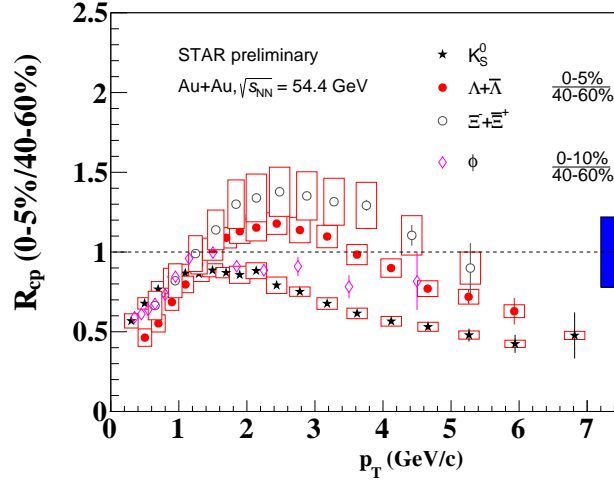


Figure 2: The nuclear modification factor, R_{CP} is plotted as a function of p_T at $\sqrt{s_{NN}} = 54.4$ GeV for K_S^0 , $\Lambda + \bar{\Lambda}$, $\Xi^- + \bar{\Xi}^+$ and for ϕ . The vertical lines represent the statistical error bars and the rectangular boxes represent the systematic error bars. Systematic errors are not shown for ϕ mesons. The blue box represents the uncertainty from the determination of the number of binary collisions.

The ratio, $N[\Omega + \bar{\Omega}^+]/2N[\phi]$ is calculated for different centralities as shown in Fig. 3. The ratio shows an enhancement at intermediate p_T and the enhancement is larger for central collisions than peripheral collisions which suggests the idea of quark coalescence hadronization [5]. The ratio at 54.4 GeV is compared with other STAR energies [6] for most central collisions as shown in Fig. 4. $N[\Omega + \bar{\Omega}^+]/2N[\phi]$ ratio shows the same trend and is consistent with other energies except for 11.5 GeV data where the larger statistical error bar restrict us from making any conclusion.

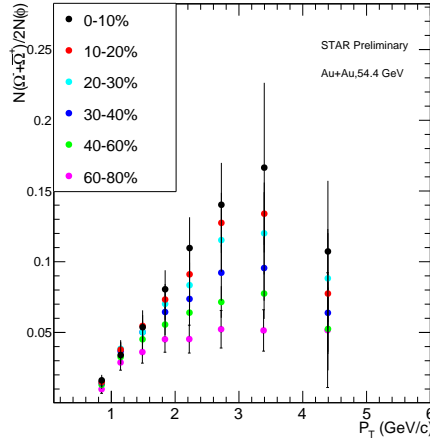


Figure 3: $N[\Omega + \bar{\Omega}^+]/2N[\phi]$ is plotted as a function of p_T for different centrality classes at $\sqrt{s_{NN}} = 54.4$ GeV. Only statistical error bars are shown.

The elliptic (v_2) and triangular (v_3) flow coefficients are measured for the strange and multi-strange hadrons for minimum bias events at $\sqrt{s_{NN}} = 54.4$ GeV as shown in Fig. 5. A mass ordering is observed at low p_T (< 2 GeV/c), where the particles with smaller mass show a higher flow

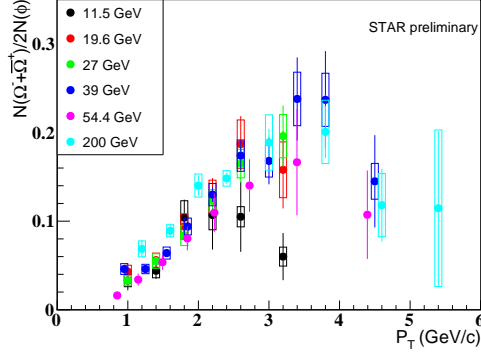


Figure 4: $N[\Omega + \bar{\Omega}]/2N[\phi]$ ratio vs. p_T for 0-10% centrality at $\sqrt{s_{NN}} = 54.4$ GeV is compared with other STAR energies for most central collisions. For 54.4 GeV only statistical errors are shown.

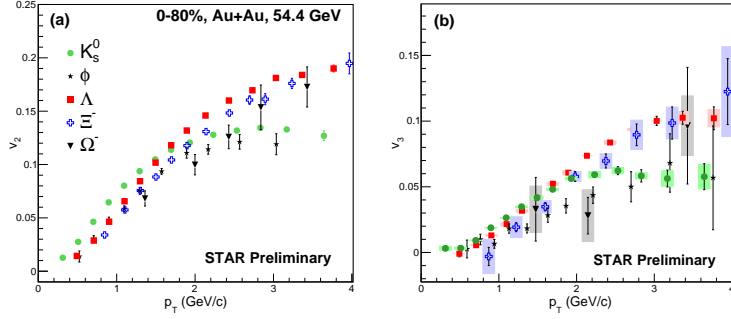


Figure 5: Left panel shows the v_2 as a function of p_T for 0-80% centrality at $\sqrt{s_{NN}} = 54.4$ GeV for K_S^0 , Λ , ϕ , Ξ^- and Ω^- . The right panel shows the same for v_3 . The vertical bars here are the statistical error bars and the shaded boxes are the systematic error bars.

which is due to the radial flow of the system during the QGP phase. A particle type dependence is observed in both v_2 and v_3 at high p_T region. We have studied the NCQ scaled v_2 as a function of NCQ scaled transverse kinetic energy at $\sqrt{s_{NN}} = 27$ and 54.4 GeV for 0-80% centrality as shown in Fig. 6. The NCQ scaled v_2 falls on a single curve for all the hadron, which indicates that the collectivity is developed during the initial QGP phase of the system. Similar behaviour is observed in case of NCQ scaled v_3 at $\sqrt{s_{NN}} = 54.4$ GeV as shown in Fig. 7.

4. Summary

In summary, we have measured the p_T spectra of strange hadrons, K_S^0 , Λ , $\bar{\Lambda}$, ϕ , Ξ^- , Ξ^+ , Ω^- , $\bar{\Omega}^+$ at midrapidity in Au+Au collisions at $\sqrt{s_{NN}} = 54.4$ GeV. The nuclear modification factor, R_{CP} for the above mentioned particles has been measured which shows a strong suppression at high p_T . The baryon to meson ratio, $N[\Omega + \bar{\Omega}]/N[\phi]$ shows an enhancement at intermediate p_T which is higher for central collisions than that for peripheral collisions. The anisotropic flow coefficients, v_2 and v_3 , have been measured as a function of p_T in 0-80% centrality for all the strange particles mentioned above. A mass ordering is observed at low p_T and a baryon to meson separation is observed at high p_T . The NCQ scaling founds to hold for both v_2 and v_3 .

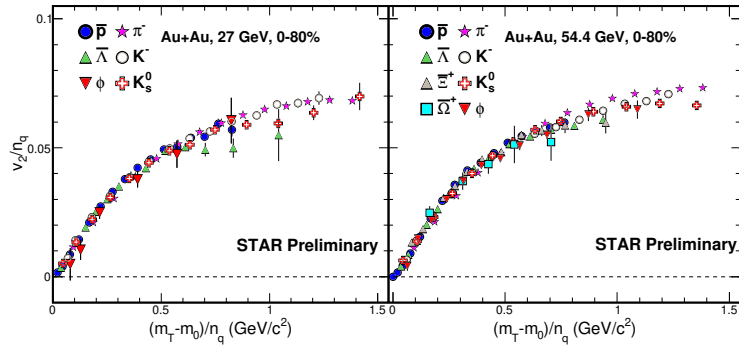


Figure 6: The left panels shows the NCQ scaled v_2 as a function of transverse kinetic energy at $\sqrt{s_{NN}} = 27$ GeV for 0-80% centrality. The right panel shows the same for $\sqrt{s_{NN}} = 54.4$ GeV. Only statistical error bars are shown.

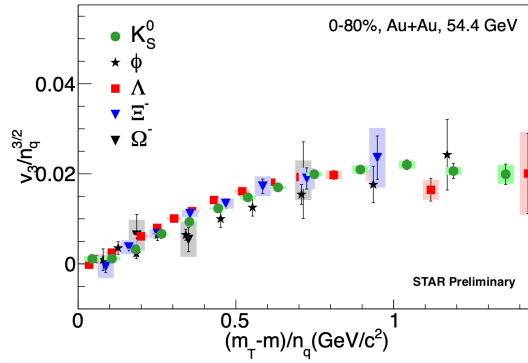


Figure 7: NCQ scaled v_3 is plotted as a function of transverse kinetic energy at $\sqrt{s_{NN}} = 54.4$ GeV for 0-80% centrality. The vertical bars here are the statistical error bars and the shaded boxes are the systematic error bars.

References

- [1] Chun Shen et al., J. Phys. G: Nucl. Part. Phys. **38**, 124045 (2011)
- [2] A. M. Poskanzer and S. A. Voloshin, Phys. Rev. C **58**, 1671 (1998)
- [3] A. Shor, Phys. Rev. Lett. **54**, 1122 (1985)
- [4] N. Borghini and J.-Y. Ollitrault, Phys. Rev. C **70**, 064905 (2004)
- [5] J. H. Chen et al, Phys. Rev. C **78**, 034907 (2008)
- [6] J. Adam et al. (STAR), Phys. Rev. C **102**, 034909 (2020)